

CASE COMPARISON BETWEEN DIRECT IMAGE COMPRESSION AND HOLOGRAM COMPRESSION

Ana-Maria SANDU¹, Nicolae MIHALE², Mihaela Andreea UNGUREANU^{2*},
Eugen I. SCARLAT²

Image compression means to encode a primary digital image in a secondary binary stream either to be stored in minimum bit-space or transmitted remotely. Starting from the “image” in the sense of a complex optical field as object for human vision and its corresponding hologram, the study presents the comparison between the genuine object and two of its copies obtained via two different sequences: one is consisting in compression-decompression of the hologram of the object followed by object retrieval, whilst the other is consisting in simply compressing-decompressing the object itself. Depending on the pathway, the compression algorithm uses spatial transforms (discrete wavelet DWT, discrete cosine DCT), or no transform at all. The performances of the two alternatives are discussed in terms of root-mean square distance (RMSD) for different quantization matrices (QM) and compression ratios (CR). The performances of hologram compression are approaching those of direct compression for visual images based on optimal JPEG techniques and might be an option for objects carrying information with no visual significance.

Keywords: hologram compression, compression ratio, Python language, wavelet, JPEG, quantization matrix, rounding factor.

1. Introduction

Computer vision applications have received a considerable attention in the last decades. Feature descriptors and detectors have been documented in literature with various definitions and approaches [1]. Generally, there are two main groups of images. One is consisting in visual images, i.e. images for human eye interpretation like in TV systems, video formats, or visual arts. The other group consists in images for automated investigation where higher processing accuracy is mandatory (e.g. barcodes and security labels, holographic stamps, fingerprints, environment textures). For the second group, human vision might not even be involved at all. Here we deal with the first group, with objects with visual significance and the (true) holograms associated thereof.

¹ CAMPUS Research Center, Doctoral School of Electrical Engineering, University POLITEHNICA Bucharest, Romania

² Physics Department, University POLITEHNICA Bucharest, Romania

*corresponding author: mihaela.ungureanu96@upb.ro

Augmented reality applications for unmanned ground vehicles also require 3-dim image acquisition of site details, traffic indicators, or neighbouring objects. Since traffic safety is the ultimate objective of such automated technologies, real time 3-dim mapping of the surrounding environment is mandatory [2]. Keeping details that exceed the human sensorial abilities and consequently a common processing capacity may improve systems security. Holography and quantitative imaging offer promising techniques for fulfilling the scope with the price of huge amounts of storing and transmitting binary data. Any saves of software memory which do not hinder the relevant information is therefore subject of research.

True holograms carry third-dimension information for high precision, automated applications like comparisons, recognition, identifying of small changes in sensitive samples [3], or to visualize 3-dim micrometric complex structures [4]. Since in digital images the neighbouring pixels are generally correlated, there is certain room to use lossless compression by removing redundancy via adequate transform like Fourier and its Cosine version, wavelet, Karhunen-Loève, etc. Depending on the scope and the characteristics of the detector thereof, additional lossy compression can be performed by neglecting the less relevant features of the images [5].

The storing techniques for visual images exploit the human vision property to be sensitive rather to small variations in brightness over large areas than to the strength of high-frequency brightness variations. Consequently, the magnitudes of the higher frequency components are less relevant and can be stored with a lower accuracy than the low-frequency components. Accordingly, subjective measures like mean opinion scores are preferred to assess the picture quality. In this respect JPEG and MPEG standards became versatile commercial techniques for storing and remotely transmitting video images [6]. In the case of images for automated investigation the details might be essential - especially when carrying true quantitative information - therefore the higher frequencies are useful as well. So far there is no standardized compression technique for them even there are efforts to adapt JPEG2000 to compressing such detailed objects like holograms [7, 8].

In this study we made computational comparisons between two ways of compressing the same object: i/ compression-decompression of the hologram of the object (way 1), and ii/ direct compression-decompression of the object (way 2). The genuine object is compared with those obtained via the processes i/ and ii/ by computing the root-mean squared distances (RMSD). The performances of processes are compared as compression ratios (CR) provided that RMSD remains below a certain threshold. Generally, the direct compression-decompression procedure (way 2) uses DWT as key step to achieve high CRs [5]. In the present computational approach, the holograms are the Fourier transforms of the objects. The approach is supported by the real cases where holograms arise naturally as consequence of propagation of light when diffracted by objects. It follows there is

no DWT or other transformation along way 1 because it would be useless to try to de-correlate even more the hologram samples by additional mathematical transformations.

Work organization is as follows: after Introduction, in Sec.2 are presented briefly some basic theoretical elements related to holograms and compression processes, in Sec.3 is presented the computational implementation, Sec.4 deals with experimental results obtained on objects with pre-defined spatial frequencies as well as on an object with visual significance labelled „vehicle”; finally the conclusions are summarized in Sec.5.

2. Theoretical framework

2.1 Holograms

Let be an illuminated object that produces the source field $Obj(x',y',z')$; its timeless equation is

$$Obj(x',y',z') = |Obj(x',y',z')| \cdot \exp(i \cdot o(x',y',z')), \quad (1)$$

where the vertical bars mean absolute value whilst $o(x',y',z')$ is the spatial phase shift, and $i = \sqrt{-1}$. If $o(x',y',z')$ is identical to zero, then the object reduces to a photography. Due to light propagation, formally stated by the diffraction operator $Prop$, the source field transforms as $\Psi(x,y) = Prop\{Obj(x',y',z')\}$ in a subsequent recording plane (x,y) . Theoretically the operator $Prop$ is the Fresnel-Kirchhoff integral across the curved surface of the object frontier. For thin objects compared to the propagation distance the output of the diffraction integral is proportional to the Fourier transform [9]. Thus the field distribution in the recording plane (the diffraction image of the object) is also a complex function with amplitude and phase

$$\Psi(x,y) = A(x,y) \cdot \exp(i \cdot \varphi(x,y)), \quad (2)$$

or, equivalently, with real and imaginary parts

$$\Psi(x,y) = \text{Re}\{\Psi(x,y)\} + i \cdot \text{Im}\{\Psi(x,y)\}. \quad (2')$$

Irrespective the representation, object information does exist in both components. The amplitude A gives the spatial harmonics whilst φ accounts for the phase shifts they overlap in each point (x,y) . If $A(x,y)$ is varying smoothly, or the shadows are not important for the representativeness of the object (e.g. they may depend on the illumination angle), then only φ remains, which often is sufficient for the recovery of Obj .

From the computational perspective, object recovery means to retrieve, up to a scale factor, the function $Obj(x',y',z')$ by de-convolving the diffracted object

$Prop^{-1}\{\Psi(x,y)\} \propto Obj(x',y',z')$. Finally $Obj(x',y',z')$ can be represented, if necessary, by a 3-dim scene. Therefore, if the complex distribution $\Psi(x,y)$ is known, then the object can be reconstituted by simulating the process $Prop^{-1}$ with the help of the deconvolution codes (inverse Fourier transform).

Experimentally, the object can be visualized (although this is not necessary in all practical applications) by illuminating the associated hologram, i.e. a print of Ψ on a suitable material substrate. The print can be either in the form of the classic intensity hologram resulting from the superposition of Ψ with a reference beam Ref (the asterisk means complex conjugation) [10]

$$H_G(x,y) = (\Psi + Ref)^*(\Psi + Ref), \quad (3)$$

or in the form of a complex hologram

$$H(x,y) = \Psi(x,y). \quad (3')$$

The latter has to be recorded as such on a material that supports simultaneous amplitude and phase recordings, e.g. amplitude and phase diffraction elements (DAEs and DPEs), combinations of them, or innovative configurations of spatial light modulators (SLMs) [11]. In both versions (3) and (3') the visualization of the object by hologram illumination is explained by those presented, for example, in [12], and relies in the fact that one of the diffracted beams - the one where the object appears - is the conjugate operator $Prop^* = Prop^{-1}$. The lacking of reference term in version (3') make it more convenient for computational implementation such that here the hologram is $H(x,y)$.

2.2 Compression procedures

The compression steps for digital video images ("objects") are as follows [5]: i/ partition of each matrix into 8×8 pixels blocks, each block being processed without reference to the others, ii/ space transformation, iii/ quantization with quantization matrix QM , iv/ rounding, using a multiplication coefficient associated to QM , v/ binary encoding. In the step ii/ the transform (Fourier or its version DCT, DWT, other) reduces the correlation among samples; DWT is preferred in the case of visual objects due to its specific filtering properties in line with the dynamic features and spectral sensitivity of the eye [13, 14]. In the case of hologram compression, the step ii/ is completely omitted since the hologram itself is a Fourier transform. In step iii/ each block is lossy compressed by quantization and rounding such that to obtain as many as possible zero elements; QM might be either Q_1 , i.e. the one recommended by JPEG for visual purposes [5], or a neutral one Q_2 (all elements equal to 1):

$$Q_1 = \begin{bmatrix} 16 & 11 & 10 & 16 & 24 & 40 & 51 & 61 \\ 12 & 12 & 14 & 19 & 26 & 58 & 60 & 55 \\ 14 & 13 & 16 & 24 & 40 & 57 & 69 & 56 \\ 14 & 17 & 22 & 29 & 51 & 87 & 80 & 62 \\ 18 & 22 & 37 & 56 & 68 & 109 & 103 & 77 \\ 24 & 35 & 55 & 64 & 81 & 104 & 113 & 92 \\ 49 & 64 & 78 & 87 & 103 & 121 & 120 & 101 \\ 72 & 92 & 95 & 98 & 112 & 100 & 103 & 99 \end{bmatrix}, \quad Q_2 = \begin{bmatrix} 1 & 1 & 1 & 1 & 1 & 1 & 1 & 1 \\ 1 & 1 & 1 & 1 & 1 & 1 & 1 & 1 \\ 1 & 1 & 1 & 1 & 1 & 1 & 1 & 1 \\ 1 & 1 & 1 & 1 & 1 & 1 & 1 & 1 \\ 1 & 1 & 1 & 1 & 1 & 1 & 1 & 1 \\ 1 & 1 & 1 & 1 & 1 & 1 & 1 & 1 \\ 1 & 1 & 1 & 1 & 1 & 1 & 1 & 1 \\ 1 & 1 & 1 & 1 & 1 & 1 & 1 & 1 \end{bmatrix} \quad (4)$$

The elements of QM control the compression ratio: larger values imply coarser quantization, more zero coefficients, and greater compression. In step v/ the data is streamed by zig-zag pathway and run-length coding, and finally by binary encoding (Huffman) that drastically reduce the memory space. CR is evaluated as the ratio of initial uncompressed memory size to the compressed memory size. Decompression uses the reverse ways dependent on hologram case or object case.

Among a lot of objective image quality metrics developed in the past few decades, the well-known $RMSD$ remains a suitable global measure in spite of the disadvantage to be insensitive to visual meaningfulness. For $L_x \times L_y$ size the distance between an object and its replica j is:

$$RMSD_j = \sqrt{\frac{1}{L_x L_y} \sum_{x,y} |Obj(x', y', z') - Obj_j(x', y', z')|^2}. \quad (5)$$

By coding the number of levels in Eq. (5) in 8 bits, the biggest distance would be:

$$RMSD_{\max} = 255. \quad (5')$$

3. Computational implementation

The fore mentioned steps i/-v/ at Chp.2.2 were implemented on a standard computer. ‘‘Hologram compression’’ is in the sense of compressing $\Psi(x,y)$ whilst ‘‘direct object compression’’ means to act upon $Obj(x', y', z')$.

3.1 Algorithm

The compression algorithm is a Python based one, developed locally and run under a versatile interface with the following facilities: programmable run of steps i/-v/, the choice of transform, QM , and rounding coefficient, as well as the option for the complex representation as amplitude-phase or real-imaginary. The process of hologram generation, propagation and reconstruction is based on previous developed codes [15, 16]. In all working modes the decompression is the same as in [17]. In this work only part of its facilities was used.

3.2 Scheme of compressions

In Fig.1 the complex matrices given by Eq. (1) are denoted "Object" while those of the corresponding holograms given by Eq.(3') are pointed out as "Hologram" by Fourier transform:

$$|Obj(x',y',z')| \cdot \exp(i \cdot o(x',y',z')) \Leftrightarrow A(x,y) \cdot \exp(i\phi(x,y)). \quad (6)$$

Depending on the element on which the compression-decompression is performed, two other versions of the "Object" are obtained: if it is done on the hologram, the result is "Object 1", whilst if it is done directly on the object, the result is "Object 2" (see way 1 and way 2 in Fig.1). Quantitatively, "Object 1" and "Object 2" are compared to "Object" using the *RMSD* measure stated by Eq.(5).

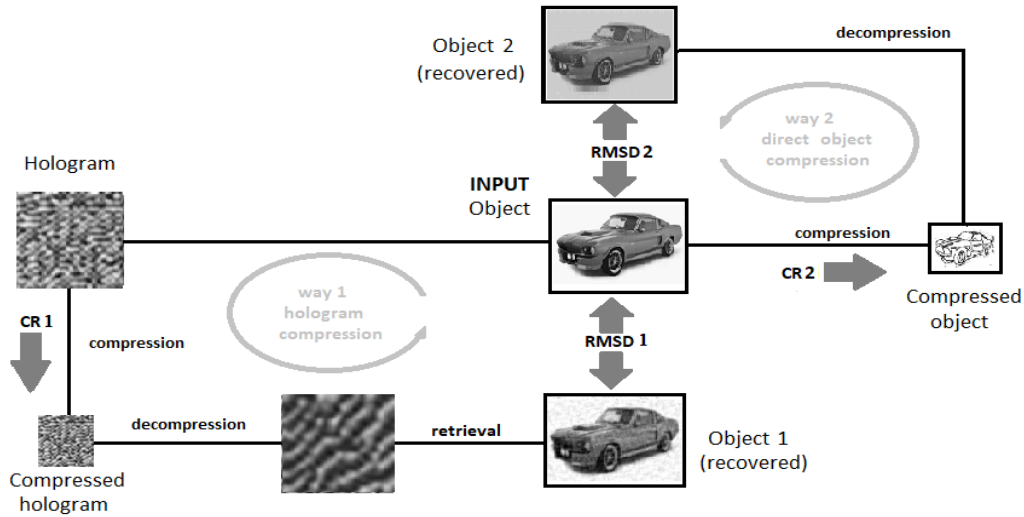


Fig.1 Scheme of the work: *CR* – Compression ratio, *RMSD* – Root-mean square distance

The working hypotheses are: 1/ the use of objects for the human visual sensor in the simplified form of a photographic image, so JPEG 2000 is accepted as optimum benchmark for the study, 2/ in the case of objects the compression procedure follows all steps i/-v/, differing from the case of holograms where the step ii/ is omitted, and 3/ the same compression algorithm is applied to both amplitude-phase (2) or to the real-imaginary parts (2') of the holograms.

4. Results

To test the adequacy of the transforms, *QMs*, and rounding coefficients, the input has been fed firstly with objects representing pure black and white chessboard-like squares processed in JPEG approach, i.e. DWT combined with Q_1

from Eq.(4), rounded at unity values. The ensemble is designed as wavelet filter that preserves the low frequencies to the detriment of the high ones, uninteresting to human perception.

Table 1


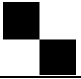
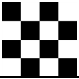
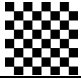
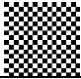

Direct object compression using DWT and Q_1						
Genuine object						
$RDMS\ 2$	0	94.7	123.5	144.4	169.5	176.5
$CR\ 2$	62.3	63.9	63.9	63.9	63.9	63.9

Table.1 shows that CR is high across the investigated spectrum. The distance between Object 2 and Object 1 is smaller at low frequencies and increases at high frequencies as expected. The latter are progressively attenuated causing the increase of $RDMS$ as frequency increases. The space periods smaller than the width of the grey lines that appear in the reconstructed objects at the borders of the squares are lost in the spectra (Fig.2b, d)).

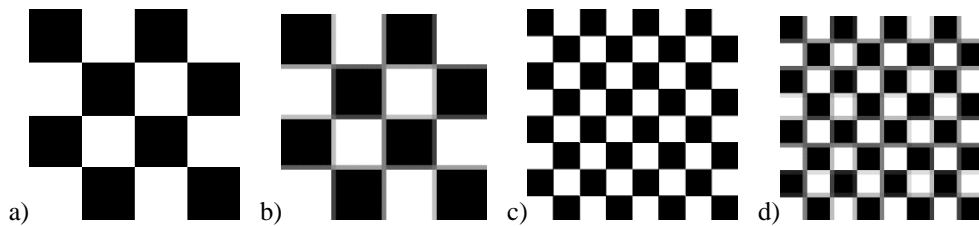


Fig.2 Objects by direct compression-decompression: genuine a), c), and recovered b), d). The grey lines at the borders of the squares is noise due to spectral losses



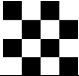
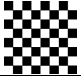


Table 1 and Fig.2 provide a useful finding for the study. The results suggest to accepting, as a reference, that the visual significance of the object is preserved up to the threshold $RMSD=144.5$, or roundly

$$RMSD_{TH}=144. \quad (7)$$

To highlight the advantage of using DWT associated with quantization matrix Q_1 we also present the results obtained with DCT associated to Q_2 (rounded to unity as well). When using the neutral matrix Q_2 all frequencies are conserved, i.e. the higher ones are no longer attenuated. Provided that Eq.(7) stands, the variation of CR with frequency, for the same spatial frequencies, is indicated in Table.2. One can remark the disadvantage of not obtaining acceptable CR at higher frequencies in spite of a good recovery (but not always desired nor necessary) of the object. For the sake of obtaining higher CR it seems logical to prefer the combination DWT- Q_1 instead of DCT- Q_2 as JPEG2000 standard does.

Table 2



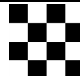



Direct object compression using DCT and Q_2

Genuine object						
<i>RDMS 2</i>	0	106.8	106.6	105.8	106.8.5	114.8
<i>CR 2</i>	62.2	51.9	34.3	20.6	10.6	5.7

The compression of the holograms associated with the same chess-like objects takes into account the hypotheses 1/-3/ stated at the end of Sec.3.2. Holograms are represented successively in the form given by Eq. (2) and Eq.(2'). Tables 3 and 4 show the results.

Table 3



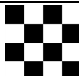
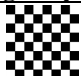
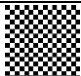
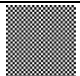
Hologram compression with Q_1 in amplitude-phase representation

Genuine object						
<i>RDMS 1</i>	0	188.9	180.2	178.8	178.8	150.1
<i>CR 1</i>	62.3	5.9	3.8	3.2	3.4	5.3

In amplitude-phase representation given by Eq.(2) *RMSD* is too large and the object is altered even at low compression ratios.

Table 4

Hologram compression with Q_1 in real-imaginary representation

Genuine object						
<i>RDMS 1</i>	0	62.9	65.3	63.8	52.5	51.4
<i>CR 1</i>	62.3	20.0	20.1	19.8	15.2	30.6

The results improve (see Table 4) in real-imaginary approach illustrated by Eq.(2'). They look better in terms of *CR* for *RMSD* under the threshold stated by Eq. (7). To drag *CR* inside an acceptable range, a coarser rounding factor of ten was used in the hologram space. The worse result in amplitude-phase representation is caused by the too severe shut down to zero of too many phase values. Since the phase samples are less correlated and therefore contain the largest part of object information [18], a lot of this is lost in the rounding step.

The results obtained by direct compression (way 2, Table 1) and by hologram compression (way 1, Table 4) are comparable in terms of *CR* and *RDMS*. Excepting the continuous term (the single square case) which behaves identically on both ways, a higher compression ratio is paid with a worse recovery of the object. Provided that the quantization matrix Q_1 was designed for visual objects, the results prove it works also when compressing the associated hologram.

For 256 levels (the rightmost column in Table 5) the reconstructed objects are shown in Fig.5 b, c.



Fig.5 Genuine object “vehicle” in 256 grey levels a), and reconstructed objects via way 1 b), and via way 2 c).

Original JPEG offers the best results in terms of *CR*. In the interval 32-256 grey levels the performances obtained by compressing the holograms are approaching the most the direct compression case. Despite the meaningfulness seems to be also better in the case of direct compression as suggested by Fig.5 a)-c), one has to remark that *RMSD* is better in the case of hologram compression. It suggests that it may be a promising tool for automated comparison where fine details are essential. A mandatory step to achieve the goal is to choose a proper *QM* according to the particular features of the investigated objects.

5. Conclusions

Hologram case appears naturally for fine objects at long distances due to the properties of the propagation of light. Hologram compression allows for object retrieval without using wavelet transform. Despite the alternatives are recommended for different practical applications, the comparison of the performances of the crude compression-decompression was analyzed in terms of compression ratio and root-mean square distance.

Direct compression with $DWT-Q_1$ and hologram compression with $_{-}Q_1$ are comparable. Although hologram compression provides a lower overall error, the compression ratio is better for direct compression, as expected since, by hypothesis, JPEG 2000 is the optimum reference. Real-imaginary representation is a better option than amplitude-phase.

Hologram compression remains an option for small objects or for objects without visual significance. The performances depend on finding an appropriate *QM* which, in turn, depends essentially on the formalization of the characteristics of the class of objects subjected to analysis. Once the scope and the associated features should have been established, the further research has to consider i/ to finding a suitable quantization matrix or a suitable combination between the quantization matrix and the type of the transformation, and ii/ to building specific codes devoted to real and imaginary parts.

Acknowledgement

The authors acknowledge the support of the Romanian Ministry of Research and Innovation, PCCDI-UEFISCDI, grant no. PN-III-P1-1.2-PCCDI-2017-0917/21PCCDI/2018 CARSafe.

REFERENCES

- [1]. *M. Hassaballah, A.A. Ali, H. Alshazly*, “Image Features Detection, Description and Matching”, in *Image Feature Detectors and Descriptors; Foundations and Applications*, Eds: A.I. Awad, M. Hassaballah, Chp.2, Springer International Publishing (Verlag), pp.11-45, 2016.
- [2]. *C. Lin, L. Li, W. Luo, K.C.P. Wang, J. Guo*, “Transfer Learning Based Traffic Sign Recognition Using Inception-v3 Model”, *Periodica Polytechnica Transp. Engin.*, **vol.47**, no.3, pp.242-250, 2019.
- [3]. *V.L. Calin, M. Mihailescu, N. Mihale, A.V. Baluta, E. Kovacs, T Savopol, M.G. Moiescu*, „Changes in optical properties of electroporated cells as revealed by digital holographic microscopy”, *Biomed. Opt. Expr.*, **vol.8**, no.4, pp.2222-2234, 2017.
- [4]. *M. Mihailescu, I.A. Paun, M. Zamfirescu, C.R. Luculescu, A.M. Acasandrei, M. Dinescu*, „Laser-assisted fabrication and non-invasive imaging of 3D cell-seeding constructs for bone tissue engineering”, *Journal of Materials Science*, **vol.9**, no.51, pp.4262-4273, 2016.
- [5]. *R. Ansari, C. Guillemot, N. Memon*, “Lossy Image Compression: JPEG and JPEG2000 Standards.”, in *Handbook of Image and Video Processing*, Elsevier Inc., pp.709-731, 2005.
- [6]. *J. Vrindavanam, S.Chandran, G.K. Mahanti, K. Vijayalaksh*, “JPEG, JPEG2000 and PBCS based Image Compression: An Experimental Analysis”, *International Journal of Computer Applications (0975 –8887)*, **vol.58**, no.10, pp.16-22, 2012.
- [7]. *S. Jiao, Z. Jin, C. Chang, C. Zhou, W. Zou, X. Li*, “Compression of Phase-Only Holograms with JPEG Standard and Deep Learning”, *Appl. Sci.*, **vol.8**, no.1258, 2018.
- [8]. *R. Corda*, “Digital Holography Data Compression”, *Telfor Journal*, **vol.11**, no.1, pp.52-57, 2019.
- [9] *E.W. Marchand, E. Wolf*, “Consistent formulation of Kirchhoff’s diffraction theory”, *Journal of the Optical Society of America*, **vol.56**, pp.1712–1722, 1966.
- [10]. *D. Gabor*, “A new microscopic principle”, *Nature*, **vol.161**, no.777, 1948.
- [11]. *J-P. Liu, W-Y Hsieh, T-C. Poon, and P. Tsang*, "Complex Fresnel hologram display using a single SLM," *Appl. Opt.*, **vol.50**, pp.128-135, 2011.
- [12]. *S. Reichelt, N. Leister*, “Computational hologram synthesis and representation on spatial light modulators for realtime 3D holographic imaging”, *J. Phys.: Conf. Ser.* 415 012038, 2013.
- [13]. *J. Oliver, M. Malumbes*, “Low-Complexity Multiresolution Image Compression Using wavelet lower trees.”, *IEEE Transactions on Circuits and Systems and Video Technology*, no.16, 2006.
- [14]. *E. Christophe, C. Mailhes, P. Duhamel*, “Adaptation of zero-trees using signed binary digit represent-tations for 3-dim image coding”, *Journ. Image Video Process.*, 2007.
- [15]. *M. Mihăilescu, L. Preda, A.M. Preda, E.I. Scarlat*, „Modified Gerchberg-Saxton algorithm for diffractive optical element image retrieval”, *UPB. Sci. Bull., Series A*, **vol.67**, pp.3-14, 2005.

- [16]. *M. Mihăilescu*, "Natural quasy-periodic binary structure with focusing property in near-field diffraction pattren", *Opt. Expr.*, **vol.12**, no.18, pp.12526-12536, 2010.
- [17]. *K. Bredies, M. Holler*, "A total variation-based JPEG decompression model," *SIAM J. Imaging Sci.*, **vol.5**, no.1, pp.366-393, 2012.
- [18] *A.V. Oppenheim, J.S. Lin*, "The importance of phase in signals", *Proc.IEEE*, **vol.69**, pp.529-541, 1981.